Cytotechnology (2014) 66:259–273
DOI 10.1007/s10616-013-9565-3

ORIGINAL RESEARCH

Evaluation of YO-PRO-1 as an early marker of apoptosis following radiofrequency ablation of colon cancer liver metastases

Sho Fujisawa · Yevgeniy Romin · Afsar Barlas · Lydia M. Petrovic · Mesruh Turkekul · Ning Fan · Ke Xu · Alessandra R. Garcia · Sebastien Monette · David S. Klimstra · Joseph P. Erinjeri · Stephen B. Solomon · Katia Manova-Todorova · Constantinos T. Sofocleous

Received: 13 September 2012 / Accepted: 10 April 2013 / Published online: 25 September 2013

Abstract Radiofrequency (RF) ablation (RFA) is a minimally invasive treatment for colorectal-cancer liver metastases (CLM) in selected nonsurgical patients. Unlike surgical resection, RFA is not followed by routine pathological examination of the target tumor and the surrounding liver tissue. The aim of this study was the evaluation of apoptotic events after RFA. Specifically, we evaluated YO-PRO-1 (YP1), a green fluorescent DNA marker for cells with compromised plasma membrane, as a potential, early marker of cell death. YP1 was applied on liver tissue adherent on the RF electrode used for CLM ablation, as well as on biopsy samples from the center and the margin of the ablation zone as depicted by dynamic CT immediately after RFA. Normal pig and mouse liver tissues were used for comparison. The same samples were also immunostained for fragmented DNA (TUNEL assay) and for active mitochondria (anti-OxPhos antibody). YP1 was also used simultaneously with propidium iodine (PI) to stain mouse liver and samples from ablated CLM. Following RFA of human CLM, more than 90 % of cells were positive for YP1. In nonablated, dissected pig and mouse liver however, we found similar YP1 signals (93.1 % and 65 %, respectively). In samples of intact mouse liver parenchyma, there was a significantly smaller proportion of YP1 positive cells (22.7 %). YP1 and PI staining was similar for ablated CLM. However in dissected normal mouse liver there was initial YP1 positivity and complete absence of the PI signal and only later there was PI signal. *Conclusion:* This is the first time that YP1 was applied in liver parenchymal tissue (rather than cell culture). The results suggest that YP1 is a very sensitive marker of early cellular events reflecting an early and widespread plasma membrane injury that allows YP1 penetration into the cells.

Keywords Liver tumor ablation · Cell viability · Apoptosis · Cell necrosis · TUNEL · P2X7 receptor · Colon cancer · YoPro-1 (YP1) · Propidium iodide (PI)

S. Fujisawa · Y. Romin · A. Barlas · M. Turkekul · N. Fan · K. Xu · K. Manova-Todorova
Molecular Cytology Core Facility, Memorial Sloan-Kettering Cancer, New York, NY, USA

L. M. Petrovic
Department of Pathology, Keck Medical Center, University of Southern California, Los Angeles, CA, USA

A. R. Garcia · J. P. Erinjeri · S. B. Solomon · C. T. Sofocleous (✉)
Interventional Radiology, Memorial Sloan-Kettering Cancer Center, 1275 York Avenue, Suite H 118, New York, NY 10065, USA
e-mail: sofoclec@mskcc.org

S. Monette
Center of Comparative Medicine and Pathology, Memorial Sloan-Kettering Cancer Center, New York, NY, USA

D. S. Klimstra
Department of Pathology, Memorial Sloan-Kettering Cancer Center, New York, NY, USA

Introduction

Colorectal-cancer liver metastasis (CLM) is one of the most common liver malignancies (Sutherland et al. 2006). Liver tumor resection remains the most effective treatment, but only a minority of patients are amenable to surgery (Chiappa et al. 2009; Hanna 2004; Lupinacci et al. 2007; Misiakos et al. 2011). Radio-frequency ablation (RFA) has evolved as a minimally invasive alternative to surgery for selected patients. During RFA, an electrode is inserted into the tumor and pulses of high-frequency current deposit thermal energy locally, destroying the tumor and surrounding margin of normal liver tissue (Gillams 2005). RFA may be as effective as surgical therapy for solitary tumors of 3 cm or smaller (Abitabile et al. 2007; Amersi et al. 2006; Gwak et al. 2011; Kim et al. 2011; Kingham et al. 2012; Siperstein et al. 2007). The 5-year overall survival rate for RFA-treated patients with CLM varies widely between 14.3 % and 55.4 % (Gwak et al. 2011; Hur et al. 2009; Kim et al. 2011). However, local tumor progression (LTP) remains a significant limitation of ablation (Mulier et al. 2008; Sofocleous et al. 2011). LTP occurrence following RFA can be as high as 60 % (Abitabile et al. 2007; Amersi et al. 2006; Kingham et al. 2012; Kuvshinoff and Ota 2002; Sofocleous et al. 2008, 2011) and has been attributed to residual tumor cells at the ablation site (Pulvirenti et al. 2001).

Unlike surgical resection, where a pathological examination is routinely performed and can unequivocally demonstrate that the margins are free of residual tumor cells, there is no standardized histological confirmation of complete ablation with tumor-free margins. PET and CT scans may be able to detect the presence of residual tumors (Liu et al. 2009), but the resolution achieved with each of these modalities is such that it is not possible to detect individual tumor cells that may survive the ablation. At present imaging modalities are unable to detect residual or recurrent tumor until weeks or months following the ablation procedure. In addition, very little is known about the histopathologic and intracellular changes in the surrounding liver tissue. Previous studies have examined tissues adherent to the electrode used for ablation (Sofocleous et al. 2004), and processed them for Hematoxylin and Eosin (H&E) and other cell viability and proliferation assays (Snoeren et al. 2009, 2011; Sofocleous et al. 2008, 2012). The techniques described require tissue fixation and processing and/or staining that cannot be completed in an expedited fashion. Therefore, this approach cannot be used as an intra-procedural indicator of complete ablation with sufficient margins creation (Wang et al. 2013). The main goal of the current study was to evaluate rapid tissue examination techniques that would permit an immediate assessment of cellular death caused by the RFA treatment. Such techniques may help significantly improve the outcomes of tumor ablation and reduce the incidence of local tumor recurrence.

YO-PRO-1 (YP1) is a nuclear marker that binds to the DNA of dying cells (Idziorek et al. 1995). Its relatively large size (630 Da) prevents this dye from penetrating the intact plasma membrane of living cells. However apoptotic processes jeopardize membrane integrity allowing YP1 to enter the cells. The mechanism involved incorporates the release of ATP and UTP molecules into the extracellular space, leading to the activation of P2X7 receptors (Virginio et al. 1999). The opening of cation channels follows, allowing entry of YP1, as well as other large molecules (Chekeni et al. 2010; Michel et al. 2000; Virginio et al. 1999). Functional activity of P2X7 receptors can influence apoptotic pathways (Chow et al. 1997), and activation of these receptors has been used to promote cell death in cancer cells (Gorodeski 2009). Recent publications indicated that P2X7 receptor activation and Ca^{2+} overload may act as a death trigger for native mouse macrophages independent of Pannexin 1 and proinflammatory caspase-1 and TLR signaling (Hanley et al. 2012; Jalilian et al. 2012; Nishida et al. 2012). YP1 positivity may be an early indicator of P2X7 receptor activation. This study focused on early cellular/intracellular changes in the ablated liver tissue surrounding the target tumor as well as in ablated normal pig liver (not involved by tumor) for comparison.

Currently, YP1 is used primarily to stain cells in culture and rarely in ex vivo or in vivo tissue samples (Chagnon et al. 2010; Kohler et al. 2010; Santos et al. 2006). However, YP1 can penetrate unsectioned, whole-mount, live tissue specimens and target dying cells from the very onset of the apoptotic process (Boffa et al. 2005). In a prior investigation, YP1 was used successfully to assess the viability of isolated pancreatic islets immediately after harvesting from deceased organ donors (Boffa et al. 2005). In addition, at least 2 prior studies have used YP1 in hepatocyte

spheroids grown in culture (Castañeda and Kinne 2000; Higashiyama et al. 2003) and have demonstrated that this dye can be used in liver cells. Based on these findings, we postulated that YP1 could also be used in human liver tissues obtained after RFA, and would thus allow an early assessment of apoptosis leading to cellular death. In the current study, we obtained tissues adherent to the electrodes used in the RFA procedure, as previously described (Snoeren et al. 2009, 2011; Sofocleous et al. 2004, 2008, 2011). Further, we performed needle biopsies from central and marginal regions of the ablation zone in an effort to collect additional tumor and surrounding liver tissue for analysis and to permit us to include cases with no tissues adherent to the electrode. Our hypothesis was that YP1 would allow detection of early intracellular events leading to cell death immediately after CLM RFA. In order to assess the YP1 expression, we performed experiments on both ablated and nonablated swine and mouse liver tissues. Finally we also performed combined evaluation of YP1 with propidium iodine (PI) in mouse liver tissue and in human CLM after RFA in an effort to further assess the nature of the hepatic cellular injury.

Methods

Human tissues

Eight CLM in 7 patients were treated with percutaneous CT-guided RFA, as previously described (Gillams 2005; Livraghi et al. 2003; Sofocleous et al. 2008, 2011; Solbiati et al. 2001). Briefly, an electrode of appropriate size was inserted to provide complete ablation with clear margins (at least 5 mm) all around the target CLM (Wang et al. 2013). All tissue fragments adherent to the electrodes following ablation were collected by washing the electrodes with warmed medium (described below). Immediately following RFA, areas of the center and marginal regions of the ablation zone were targeted using CT imaging. Core biopsy samples from these regions were collected using 18–20 gauge needles. All specimens collected were maintained live in warmed culture medium [Dulbecco's Modified Eagle's (DME) medium with 15 mM HEPES (4-(2-hydroxyethyl)-1-piperazineethanesulfonic acid) buffer and 10 % fetal bovine serum (FBS); (all materials from Fisher Scientific, Pittsburg PA, USA)] and were stained with YP1 as described below.

Pig liver tissues

All procedures were performed in accordance with a protocol approved by our Institutional Animal Care and Use Committee (IACUC). Livers from 2 pigs were ablated using the same technique as for human CLM. Within 30 min after ablation, animals were euthanized by barbiturate overdose; liver tissues at the ablation site as well as those from a nonablated lobe were dissected out within 15 min of euthanasia and stained immediately with YP1 and Hoechst 33342, as described below.

Mouse liver tissues

All procedures were performed in accordance with a protocol approved by our IACUC. Mice were euthanized by avertin overdose. Liver tissue was dissected out and immediately stained with YP1 and Hoechst 33342 as described below. The liver lobe was either sectioned into small pieces before staining ($n = 6$ animals) or purposefully kept intact throughout the staining and imaging procedures ($n = 4$ animals). In order to evaluate and compare the organ-specificity of YP1 staining, tissue pieces from lung, intestinal smooth muscle, and testicular seminiferous tubules were excised from healthy adult mice ($n = 5$ animals) and stained for YP1 and Hoechst 33342 as described below.

Live staining with YO-PRO-1

Collected samples were placed in the staining solution prewarmed to 37 °C. The solution contained the following components: DME medium (Fisher Scientific) with a 15 mM HEPES buffer (Fisher Scientific), 10 % fetal bovine serum (FBS, Fisher Scientific), 10 μg/mL of Hoechst 33342 (Sigma, St. Louis, MO, USA), 0.1 μM YP1 (Invitrogen, Carlsbad, CA, USA), and the solution was filtered through 0.22 μm filter (Fisher Scientific). Hoechst 33342 served as a counterstain, labeling all nuclei. Samples were incubated in a cell culture incubator at 37 °C with 5 % CO_2 for 30 min. After 3 washes in DME with 10 % FBS, the samples were mounted for imaging.

Confocal microscopy

Stained samples were placed in a delta-T dish (Fisher Scientific). Imaging was achieved within an environmental chamber (Tokai Hit, Shizuoka-ken, Japan) mounted onto a Leica TCS AOBS SP2 with a DMIRE2 inverted microscope (Leica Microsystems, Wetzlar, Germany) with a 20×/0.7 water immersion objective with a digital zoom of 1.0–2.0. 405 nm laser line was used to excite Hoechst 33342 and 488 nm laser line for YP1. Optical z-stacks were taken with optimal settings such that non-saturated, nuclear YP1 signals could be detected with minimal background.

Tissue processing and histological staining

The samples were fixed in 4 % paraformaldehyde in phosphate buffer saline (PBS) for 10 min at 4 °C, either immediately following tissue collection or after live staining and imaging. After washing, samples were paraffin-embedded, sectioned into 5 μm slices, and processed for a TUNEL assay, as previously described (Manova et al. 1998). Briefly, the slides with sections were treated with 20 mg/mL of Proteinase K (Sigma Aldrich, St. Louis, MO, USA), followed by overnight incubation in 0.5 mL of biotin-dUTP and 100 units of TdT mixed in 100 mL of TdT buffer (TdT Staining Kit, Roche Applied Science, Indianapolis, IN, USA). The signal was visualized using Vectastain ABC Elite Kit (Vector Laboratory, Burlingame, CA, USA) and DAB reaction. A subset of tissues was immunostained with anti-OxPhos antibody (Invitrogen, Carlsbad, CA; 2 μg/mL), using a Discovery XT processor (Ventana Medical Systems, Tucson, AZ, USA). The stained slides were digitally scanned using a Mirax Scan (Carl Zeiss, Oberkochen, Germany) with a 20×/0.8 NA objective.

YO-PRO-1 penetration in mouse liver

To determine how quickly liver tissues become sensitive to YP1 staining, a mouse liver lobe was cut in half. One half was fixed immediately while the other half was kept in the incubator for 30 min before fixing. The samples were then analyzed with a TUNEL assay. In another experiment, freshly dissected mouse liver tissue was placed immediately in the environmental chamber of a confocal microscope. After initial imaging, YP1 dye was added to the medium and additional images were obtained.

Organ-specificity of YO-PRO-1 expression in other mouse tissues

In order to determine the impact of dissection on YP1 penetration in different tissues, we applied YP1 staining on organs other than the liver. The staining procedure was exactly the same as that used for mouse, human and pig liver samples.

YO-PRO-1 and propidium iodide experiments

We stained mouse liver tissues, HeLa cells and ablated CLM samples to compare YP1 with PI, a known marker of cellular necrosis, similarly to what has been previously performed in tissue cultures (Gawlitta et al. 2004). YP1 solution was prepared and applied according to our protocols described above. PI was used at a concentration of 10 μM in the same medium. 250 nM MitoTracker Red was added to HeLa cell samples.

HeLa cells and mouse liver samples

The cells and the liver tissues were incubated with YP1, PI or YP1/PI combined and imaged in 5–10 min intervals for a total period of 30 min.

Alternatively, HeLa cells and liver tissues were incubated with the fluorophores for 30 min, washed and then imaged.

Ablated human liver samples

All ablated human liver samples were incubated for 30 min in YP1 or PI solution, washed and imaged.

Image and statistical analyses

Maximum projection images from the confocal z-stacks obtained from live samples and scanned images of histologically stained samples were analyzed using Metamorph (Molecular Devices, Downingtown, PA, USA) software. The appropriate threshold was set for each image and the proportion of YP1-positive cell nuclei was calculated. Standard

error of the mean and Student's *t* test were performed in Microsoft Excel.

Results

YO-PRO-1 staining in ablated human colon cancer liver metastases

Figure 1a shows representative images of removed human liver tissue following ablation, as collected from an electrode. The tissue was stained and imaged live for YP1 (green) and Hoechst 33342 (blue). All cells in the sample were positive for YP1, indicating changes in plasma membrane permeability. The thermal injury generated by the ablation has grossly distorted the morphology of the tissue: most of the nuclei appeared extremely elongated (Fig. 1a, arrow), and nuclear and cytoplasmic regions of the cell could not be well distinguished (Fig. 1a, arrowhead), suggesting that the cells are no longer compartmentalized. Visually, the tissues appeared brown in color, as would be expected from the thermal effects of RFA. YP1 staining as well as morphological examination demonstrates that the majority of tissue adherent to the electrode was destroyed by the ablation.

Liver biopsy tissues from the central region of the ablated area contained cells with large, round nuclei that were morphologically identified as hepatocytes (Fig. 1b). The cytoplasm of these cells was intact, as demonstrated by an unstained area around the nucleus. A high proportion of Hoechst 33342-stained nuclei were positive for YP1 (96.0 ± 2.2 %), suggesting that cell membrane permeability occurred in nearly all cells. However, in this region the thermal effect on the overall morphology of the cells is not as apparent. In the marginal region as in the central region, morphologically intact hepatocytes were observed. YP1 positivity was detected in 89.8 ± 2.9 % of Hoechst 33342-stained nuclei in the margin (Fig. 1c).

We additionally wanted to validate the YP1 data with a histochemical TUNEL assay, which detects fragmentation of DNA within apoptotic cells. All samples from a single patient were fixed and stained for TUNEL. It was found that in contrast to the YP1 findings the TUNEL assay revealed that samples from the central area of ablation and those from the margin contained significantly fewer positive cells (16.5 ± 2.3 %) ($t = 20.38$, $p < 0.01$, Fig. 1d). In addition, the tissues collected were immunostained with anti-OxPhos antibody, which binds to active mitochondria in viable cells; a representative image (Fig. 1e) shows that the majority of cells were positive for the OxPhos antibody, a finding that also raised questions about the significance of YP1 staining.

Comparisons among the 3 staining experiments performed on adjacent sections of single tissue samples indicated that a large proportion of YP1-positive cells obtained from both the margin and the center of the ablation zone were negative for TUNEL and positive for OxPhos. These results suggest that plasma membranes of liver cells are compromised, allowing YP1 to enter. However, these cells remained metabolically active and without fragmentation of their DNA.

YO-PRO-1 staining in ablated and nonablated pig liver

In order to better understand the specific effect of RFA on liver cell membrane integrity in relation to YP1 positivity, we obtained tissue from both the ablated (Fig. 1f) and nonablated lobes (Fig. 1g) of swine livers. Both RFA and staining procedures were exactly the same as those used for human samples. YP1 was present in 93.5 ± 1.9 % of cells from the ablated lobe and 93.1 ± 1.9 % of cells from nonablated lobe ($t = 0.17$, $p = 0.9$). The high YP1 positivity in nonablated swine liver showed that ubiquitous YP1 expression can be caused by interventions other than RFA.

YO-PRO-1 staining in healthy adult mouse liver tissue

To further analyze the ubiquitous YP1 staining in liver tissues, we studied healthy, nonablated adult mouse liver tissues. Mouse organs could be more easily obtained as well as manipulated than swine livers. As seen in Fig. 2a, mouse samples produced results remarkably similar to those obtained with pig liver, as there was YP1 positivity in the majority of cells (65 ± 7.2 %). Closer inspection showed that live cells identified morphologically as not being hepatocytes were often void of the YP1 signal (Fig. 2b, arrows). Large, round nuclei of hepatocytes were more likely to

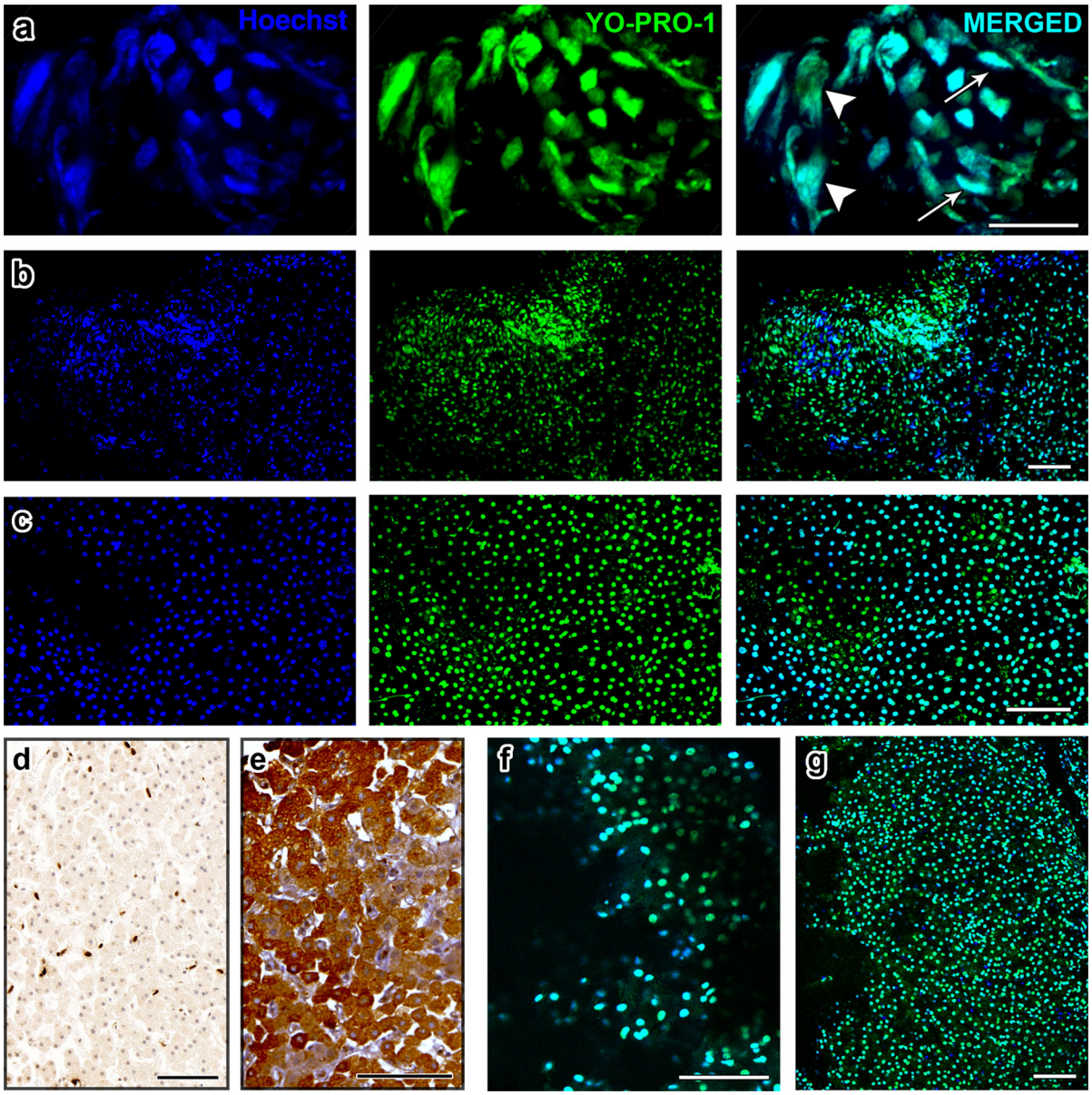

Fig. 1 Human and pig RFA liver tissues exhibit ubiquitous YO-PRO-1 staining. Projection images were compiled from confocal z-stacks of human liver sections stained live with YO-PRO-1 (*green*, center panel) and Hoechst 33342 (*blue*, left panel). The right panel shows the merged images: **a** In tissues adherent to the RFA electrode, we observed a prominent heat artifact in which some nuclei were unnaturally elongated (*arrows*). Distinct nuclear and cytoplasmic regions are not well discernible, suggesting decompartmentalization of the cells (*arrowhead*). **b** In this sample from the center of an ablated region, morphologically intact hepatocytes are observed. A high proportion is YO-PRO-1 positive. **c** In this sample from the marginal region, an area in which we expected cell survival, we also observed high YO-PRO-1 positivity. **d**, **e** A subset of the margin sample was fixed and stained with TUNEL (**d**) and anti-OxPhos antibody (**e**). We observed significantly less TUNEL signal compared to YO-PRO-1, and abundant OxPhos signal compared to YO-PRO-1. These findings suggest that despite YO-PRO-1 positivity, the margin tissue contained metabolically active cells with intact DNA. **f**, **g** YO-PRO-1 staining of ablated (**f**) and nonablated (**g**) pig liver tissues shows that RFA does not influence the amount of YO-PRO-1 positivity. *Scale bars*: **a** = 25 μm, all others = 100 μm

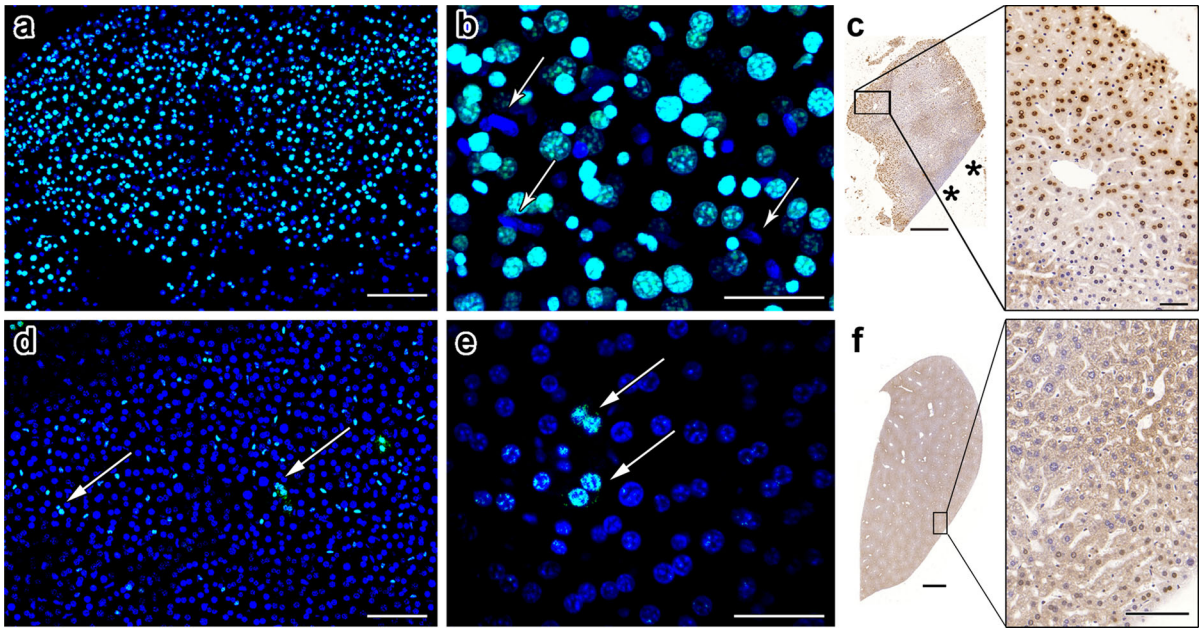

Fig. 2 YO-PRO-1 positivity in adult mouse liver tissue is influenced by the amount of physical damage inflicted during dissection. **a** A section of liver from an adult mouse was stained with YO-PRO-1 and Hoechst 33342. Exhibiting a general similarity to what was seen with human samples, a majority of the liver cells are YO-PRO-1-positive. **b** A higher magnification image reveals that nonhepatic cells with elongated nuclei seem to avoid YO-PRO-1 penetration (*arrows*). **c** TUNEL staining of mouse liver tissue shows that cells near sites of physical damage are particularly susceptible to apoptosis. We know that this is not an edge effect since TUNEL positivity is not observed near intact edge of the tissue (*asterisks*). **d**, **e** An entire lobe of liver was dissected gently and stained and imaged while intact. The proportion of YO-PRO-1-positive cells was significantly less and these cells formed small clusters (*arrows*). **f** TUNEL staining of intact liver lobe shows minimal apoptosis. *Scale bars*: **a** = 100 μm, **b** = 40 μm, **c** = 500 μm, 50 μm, **d** = 100 μm, **e** = 50 μm, **f** = 1 mm, 100 μm

be positive for YP1, compared with such smaller cells as sinusoidal endothelial cells with elongated nuclei (data not shown). However, a more precise in situ molecular analysis would be necessary before we would be able to characterize those cell types that are exempt from YP1 penetration.

TUNEL staining of mouse liver samples showed 14.9 ± 1.9 % positive cells, a significantly smaller proportion compared with the finding of YP1 staining. The signal was confined to regions near the dissected edges of tissues (Fig. 2c). When TUNEL analysis was performed within 200 μm of damaged edges, the proportion of positive cells increased to 21.1 ± 0.8 %. Farther into the tissues, the result was 8.7 ± 2.2 % positive for TUNEL, significantly lower than that near the damaged edges ($t = 5.67$, $p < 0.01$). Similarly low levels of TUNEL positive cells were observed near the intact surfaces of liver lobules (Fig. 2c, asterisks). This is in contrast to YP1 data, where we observed positive cells more than 200 μm away from the injured area.

Limited and discrete YO-PRO-1 signal in intact mouse liver

We then postulated that liver tissue may be extremely sensitive to mechanical damage caused during dissection. To test this hypothesis, a lobe of mouse liver was kept intact during extraction, staining, and imaging. The whole liver sample exhibited YP1 positivity in a very small subset of cells, generally those located in discrete, small clusters (Fig. 2d, e). The proportion of YP1 positive cells in intact liver was 22.7 ± 4.6 %, significantly less than data from dissected liver pieces ($t = 2.03$, $p < 0.01$). It is possible that intact liver covered by a capsule does not allow the penetration of YP1. Therefore, we also conducted a TUNEL assay on fixed and sectioned tissue; and we observed that the

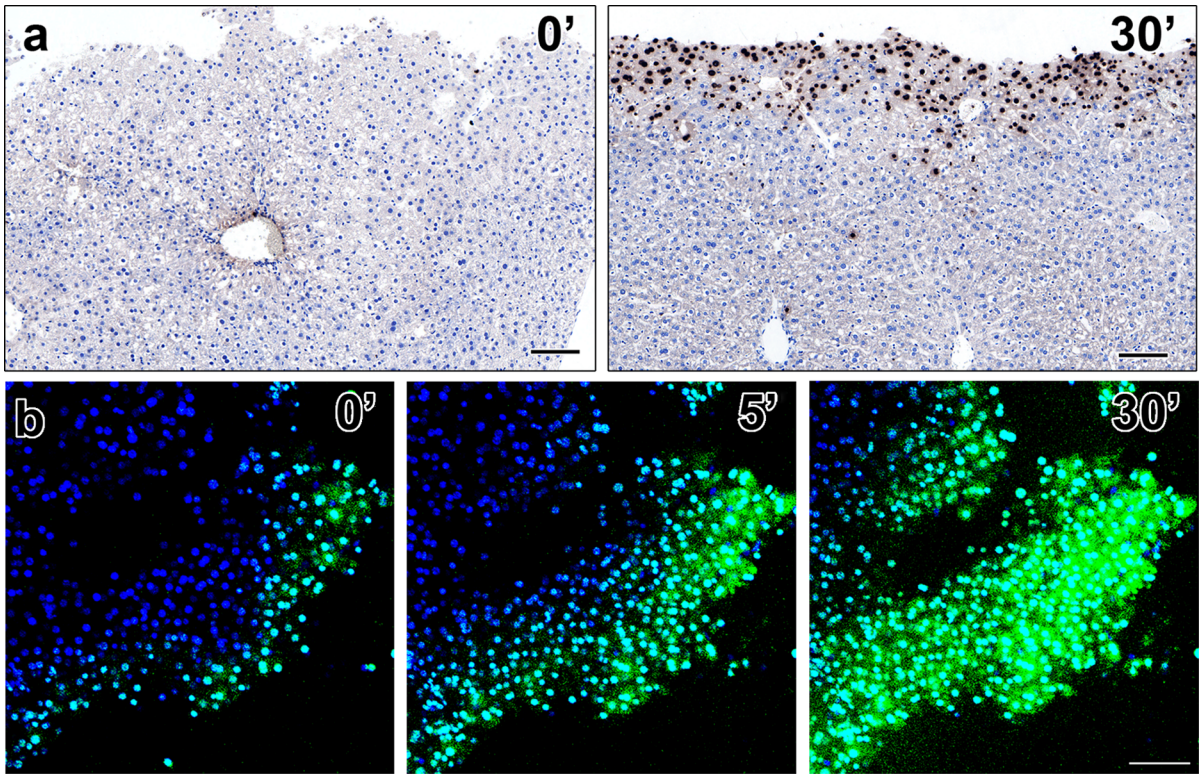

Fig. 3 A dissected liver tissue rapidly becomes positive for TUNEL and YO-PRO-1. When a dissected liver sample was fixed immediately following dissection, the tissue is void of TUNEL positivity (**a**, left panel). However when kept in the incubator for 30 min prior to fixation, the sample became positive for TUNEL staining near the cut edge (**a**, right panel). A time-lapse experiment in which YO-PRO-1 dye was added during imaging on confocal microscope showed that within 5 min the majority of cells became YO-PRO-1 positive **b**. *Scale bars*: **a** = 100 μm for both panels, **b** = 100 μm for all panels

cell death signal was virtually nonexistent in liver that had been excised and fixed while intact (1.7 ± 1.1 %, Fig. 2f).

Rapid increase in YO-PRO-1 sensitivity in unfixed mouse liver tissues

When liver samples were fixed immediately after dissection, the TUNEL signal was found to be minimal (Fig. 3a, left panel). However, if the sample was kept in medium inside a tissue culture incubator for 30 min before fixation, prominent TUNEL staining was observed near the edge of the dissection (Fig. 3a, right panel). When YP1 dye was added to dissected liver tissue placed directly on a microscope stage incubator, we observed that cells near the edges immediately became positive. During 30 min of imaging, an increasing number of cells farther and farther from the edge became YP1 positive (Fig. 3b). Based on these findings we postulated that not only mechanical damage but a dissection of an intact lobe may lead to activation of signals, affecting the normal functions of the hepatocyte plasma membrane leading to increase permeability.

The organ-specificity of YO-PRO-1 positivity in other mouse tissues

We further wanted to determine whether extraction and dissection can result in YP1 positivity in organs other than the liver. Experiments on mouse lung, intestinal smooth muscle, and testicular seminiferous tubules showed that selective subsets of cells stained with YP1 (Fig. 4). The proportion of YP1 positive cells were 72 ± 7.8 %, 52.6 ± 15.1 %, and 41.7 ± 9.1 %, respectively.

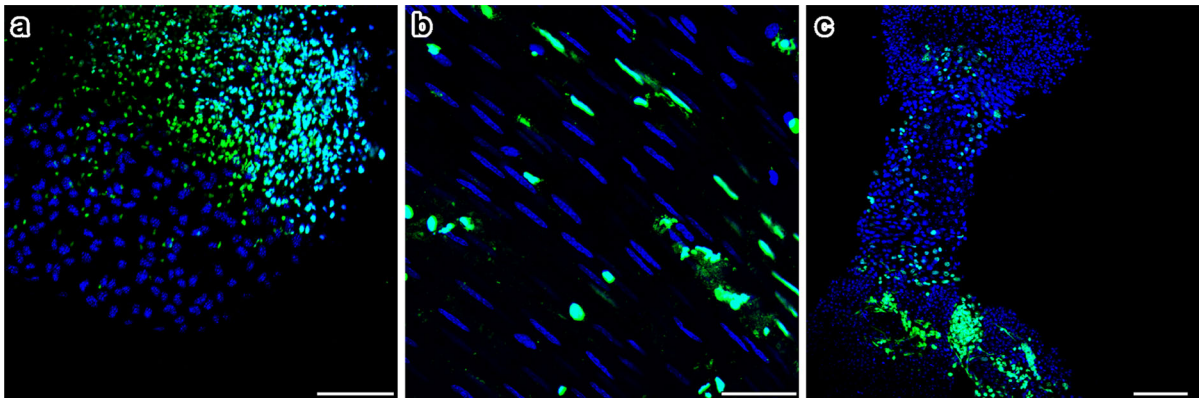

Fig. 4 Mouse non-liver tissues show distinct subpopulation of YO-PRO-1-positive cells that are largely exclusive from MitoTracker-positive cells. Tissues from lung **a**, intestinal walls **b** and seminiferous tubule **c**: each exhibit different proportions of apoptotic YO-PRO-1-positive cells. The results demonstrate the ability of YO-PRO-1 dye to specifically bind to metabolically inactive dying cells in tissues other than liver. *Scale bars*: **a** = 100 μm, **b** = 50 μm, **c** = 100 μm

YOPRO-1 (YP1) and propidium iodide (PI) experiments

Mouse liver

After 10min incubation in YP1, we observed positive cells along the tissue edge and a few others in the center of the tissue. However, the overall number of cells permeant to YP1 was limited. Significantly lower numbers of cells became positive for PI during the same time periods. Imaging during a 30 min period showed gradual increase of positive cells for both YP1 and PI and at the end, almost all cells became YP1 positive, while PI penetrated smaller number of cells (Fig. 5a, b). Similar was the result obtained from liver tissues, incubated for 30 min, washed and then imaged. Ablated human liver samples were characterized by ubiquitous YP1 and PI staining indicating permeability of cellular membranes as a result of the ablation (Fig. 5c).

HeLa cells

YP1 stained very few cells. Addition of MT red confirmed that the majority of the cells, impermeable to YP1 have functional mitochondria (MT red staining). PI penetrated the nuclei of very few cells. Double YP1/PI staining gave similar result. Cells stained either with YP1 or with PI. Double stained cells were extremely rare.

Ablated human liver samples

YP1 and PI used singly and combined stained all ablated samples of human hepatocytes.

No tumor could be distinguished morphologically.

Discussion

In the current study, we studied cell death immediately after RFA. Unlike prior studies that evaluated tissues extracted on the RFA electrode with immunohistochemical methods that usually require lengthy processing (Sofocleous et al. 2004, 2008, 2011, 2012), we used a green fluorescent dye, in which the incubation period can be as short as 5 min. With such procedure, the specimen can be viewed under the microscope within 30 min from the tissue collection. Such a rapid evaluation is critical to assess the presence of dead or viable tissue in the ablation zone depicted by radiological imaging. Lack of cell death or identification of viable tumor cells in the ablation zone would allow additional therapy that might improve oncological outcomes after liver tumor ablation.

We observed high YP1 positivity in ablated as well as non-ablated tissues from human, pig and mouse livers. These findings indicated that the YP1 signal does not represent cellular death resulting specifically from the ablation. Further, the relatively low levels of YP1 signal in organs other than liver indicate that there may be an organ specific penetration of YP1.

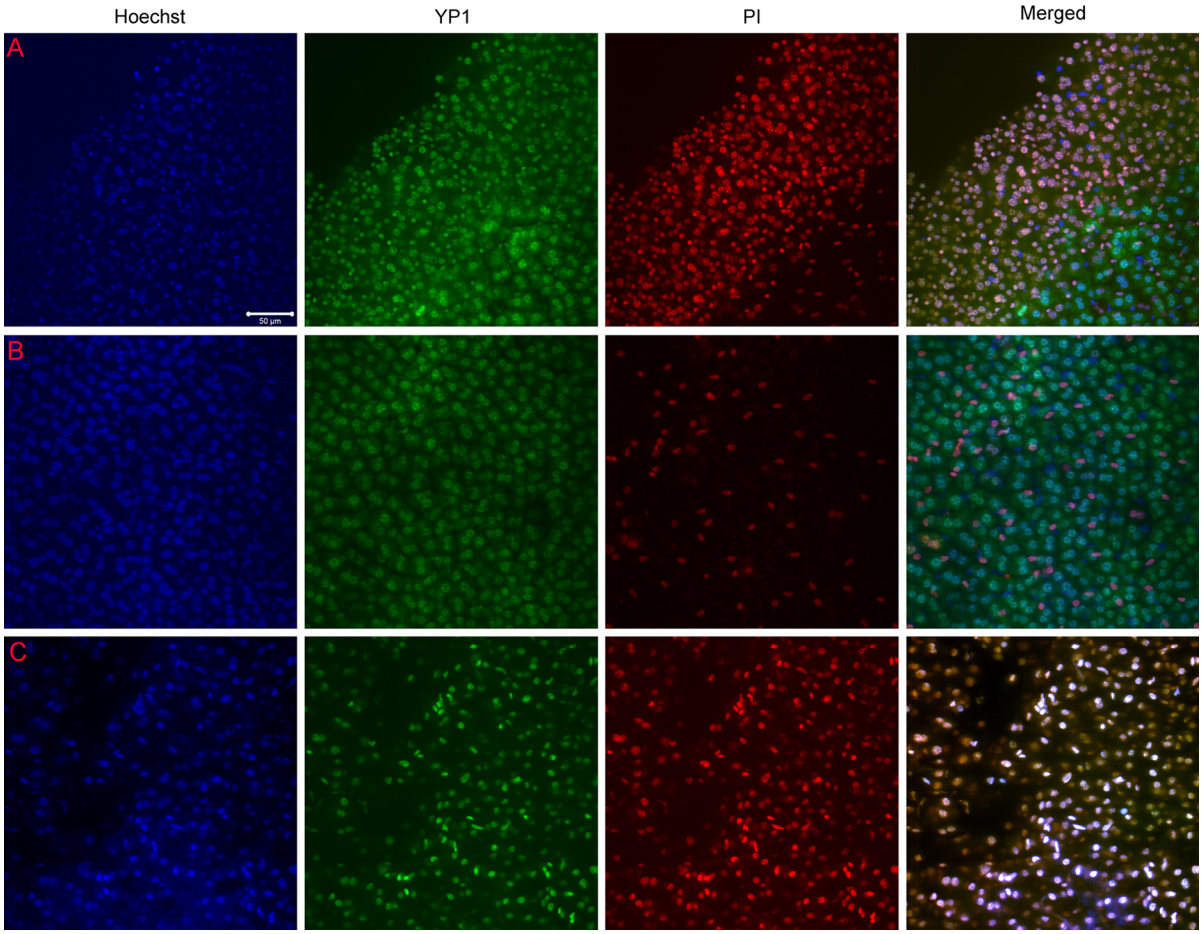

Fig. 5 The penetration of PI is slower than that of YP1 in healthy mouse liver, as opposed to RFA patient samples. **a** The edge of the healthy mouse liver sample shows a large number of both YP1 positive and PI positive nuclei with YP1 staining appearing earlier and covering more of the sample after 30 min of incubation. **b** Relatively intact healthy mouse liver shows significantly higher YP1 than PI signal, indicating that membrane pores allowing YP1 penetration can occur very early after any manipulation of the hepatocytes even in absence of mechanical damage to the tissue. **c** The human RFA patient sample shows ubiquitous YP1 and PI staining in all cells regardless of the size or location in the sample. This is most likely an indication of advanced injury and irreversible apoptosis due to the ablation treatment

The cause of the discordance between cell death markers (TUNEL) and cell-permeability markers (like YP1) remains unclear. It is possible that in the liver, the dye is taken-up non-specifically by both injured but viable as well as by apoptotic cells. Alternatively, liver cells may be highly sensitive to any manipulation (i.e. biopsy, dissection), and undergo apoptosis immediately, as detected by YP1. It appears that YP1 is a very sensitive marker of early cellular events. It is also possible that the transient activation of the plasma membrane can be a death trigger independent of pro-inflammatory caspase-1 and TLR signaling. Alternatively, liver cells may be highly sensitive to any manipulation and undergo early cellular changes (increased plasma membrane permeability) and will subsequently undergo cell necrosis possibly via different pathways (Emmett et al. 2008; Xiao et al. 2012). Small deviations from the norm cause fast responses, executed very efficiently by the hepatocytes. YP1 detects early phases of the apoptotic process in the liver, while TUNEL and cleaved caspase-3 activation report later phases in the process. The molecular components needed for propagation of warning signals and execution of fast responses, such as P2X receptors and Pannexin 1 are abundant constituents of the hepatocyte membrane (Emmett

et al. 2008; Xiao et al. 2012). Coordinated activation of P2X receptors and Pannexin1 results in diverse arrays of membrane trafficking events, including opening of pores in the membrane, allowing large molecules, such as YP1 to enter cells (Iglesias et al. 2008; Qu et al. 2011; Xiao et al. 2012). This observation may explain the discordance between cell death marker TUNEL and cell-permeability marker YP1 in the current study. The liver cells are highly sensitive to any manipulation (i.e. biopsy, dissection) and activate the process of apoptosis immediately, as detected by YP1 whereas the cells may still be viable with active mitochondria and no TUNEL activation.

From as early as 1996, YP1 has been used to label lysed cells in vitro (Gohla et al. 1996), and rarely in other types of samples. To the authors' knowledge, this dye has never been used to detect cell death in freshly removed liver tissues. Therefore, the validity and specificity of using YP1 on liver tissues has not been assessed. Boffa et al. (2005) used YP1 in the evaluation of apoptosis in pancreatic islets that were harvested and isolated from human cadaveric organs. Chagnon et al. (2010) added YP1 directly to lung tissues within anesthetized mice to study cell survival following acute lung injury. YP1 staining performed in gastric glands, pieces of dissected skin, and isolated retina samples from mice and rats has resulted in the identification of a clear distinction between live and apoptotic cells (Ito et al. 2010; Kohler et al. 2010; Liao and Puro 2006). Other investigators have cultured hepatocyte spheroids and convincingly determined apoptotic cells using YP1 (Castañeda and Kinne 2000; Higashiyama et al. 2003).

In our study, cells positive for YP1 also stained positive with OxPhos antibody, a marker of metabolically active mitochondria. The result may indicate that YP1 is taken-up by viable cells, or that YP1 is so sensitive that it labels cells that are still metabolically active but that have compromised plasma membranes. These cells may be destined to die, but have not reached the stage where the mitochondria are metabolically inactive. Similarly, TUNEL staining was present, but not as widespread as YP1. This may suggest that YP1 detects the liver cells in earlier stages of apoptosis; cells in which DNA fragmentation has not yet occurred. Prior series have shown that TUNEL positivity was significantly higher 24–72 h after treatment, compared to immediately after the ablation (Goldberg et al. 2000; Morimoto et al. 2002; Rai et al. 2005). It remains unknown whether cells that allow YP1 permeability will eventually undergo TUNEL positive cell death, or whether these cells will manage to recover, avert DNA fragmentation, and survive the insult.

It is unknown whether the process of dissection induces P2X7 receptor activation (Michel et al. 2000), but YP1 enters the hepatocytes with ease upon liver dissection. The cellular insult triggered by the physical damage occurs rapidly. When the tissues were kept alive in the incubator for 30 min prior to fixation, the extent of YP1 and TUNEL positive cells dramatically increased. We believe that this is a liver-specific phenomenon, as is demonstrated by the specific and discrete YP1 staining that has been achieved in other organ tissues and by previous studies that have used YP1 to successfully identify apoptotic cells (Boffa et al. 2005).

Why are liver tissues so vulnerable to physical damage? One reason may be due to the P2X7 receptors present in hepatocytes (Emmett et al. 2008; Taylor and Han 2010). Physical dissection may cause the release of ATP into the extracellular matrix, resulting in hyperactivation of P2X7 receptors. However, reports show that P2X7 receptors are also expressed in the lung and intestine, but not in seminiferous tubule cells (Lee et al. 2000; Mishra et al. 2011). It is unclear if P2X7 receptors in the liver are more sensitive to activation or if dissection releases extracellular ATP in greater amounts in liver compared to other organs or if some other process is responsible for our observations.

As with many other organs, separation from their natural environment induces apoptosis in liver cells. Smets et al. (2002) demonstrated in primary mouse hepatocytes that anoikis, cell death due to detachment, is a major problem during liver cell transplantation. In the current study, individual hepatocytes were not isolated from dissected liver tissue, so only the cells near the resected edges should undergo anoikis. Our time-lapse experiments did demonstrate YP1 and TUNEL signals first appearing along the resection edges and subsequently spreading into the tissue. Liver may be extremely sensitive, such that regional anoikis quickly leads to tissue-wide apoptosis. Anoikis-resistance in cancer metastasis has been investigated (Horbinski et al. 2010), however there is no prior evidence showing a particular or specific vulnerability of liver parenchyma to anoikis. This study suggests that hepatocytes, in particular, may be vulnerable to dissection, since we detected the nuclei of cells that may be endothelial cells, to be negative for YP1.

Our pig liver data are similar to those reported before by Rai et al. (2005) where liver samples were collected from pig livers post RFA and biopsies processed for TUNEL staining. Significant signal was found only 5 days post ablation, specifically in the zone close to the necrotic area. Furthermore according to recent publications P2X7 receptor activation and Ca^{2+} overload may act as a death trigger for native mouse macrophages independent of Pannexin 1 and proinflammatory caspase-1 and TLR signaling (Hanley et al. 2012; Jalilian et al. 2012; Nishida et al. 2012).

When evaluating the results of our PI and YP1 experiments it appears that YP1 penetration preceded PI entry in the hepatocytes despite the similar molecular weight of PI and YP1 (around 660 Da). The delay in PI penetration, compared to YP1 in mouse liver following dissection could indicate a specific permeability of hepatocellular membranes that may be related to early apoptosis. YP1 signal related with early apoptosis as a result of Staurosporine addition to C2C12 cell cultures has been shown (Gawlitta et al. 2004; McArdle et al. 1999) and it persisted into late apoptosis when procaspase activation and TUNEL signal were observed (McArdle et al. 1999). As a matter of fact, this study indicated that C2C12 apoptosis, induced by staurosporine, can be monitored by YP1 staining, at least 5–6 h before definite cell death (defined from PI labeling) commences. The described dual staining method (YP1 and PI) presented in that study could differentiate between two consecutive stages of cell death. These observations can explain our YP1 signal identification despite absence of TUNEL activity and in the face of mitochondrial activity. Even if the non-physiological conditions such as liver dissection cause opening of large pores (with the presumptive activation of P2X7R and Panx1), YP1 precedes PI entry. This trend was also reported for C2C12 murine skeletal muscle fibroblasts grown in 2D and 3D cultures. Staurosporine induced apoptosis was detected 2–3 h post treatment by YP1 staining and 8 h later some of the YP1 positive nuclei acquired PI positive signal signifying a transition from apoptosis to necrosis (Gawlitta et al. 2004).

The human RFA sample showed predominantly double (YP1 and PI) positive cells. The RFA procedure is supposed to create protein denaturation and coagulation necrosis This may be related with increased membrane permeability and a faster progression from early apoptosis (YP1 signal) to necrosis (PI signal) and therefore a higher degree of simultaneous dual staining than what has been previously described in C2C12 cell cultures (Gawlitta et al. 2004). It is imperative that further studies using membrane component specific markers, blocking reagents, electrophysiogy or Ca^{2+} imaging are necessary to help unravel the complexity of the occurring changes. The current study indicates that YP1 is a very sensitive marker of early cellular pro-apoptotic events. Some of the early events may be transient, as part of the yet undefined "find me" signals, or alternatively they may take different pathways resulting in cell death. In conjunction with activation of the P2X7 receptors, as it has been already shown in melanoma cells (Hanley et al. 2012), for example, one could postulate that by mediating apoptotic actions of extracellular nucleotides this may have a potential role in clinical practice as a novel therapeutic target. It also appears that the hepatocytes are more sensitive and susceptible to these early intracellular events leading to apoptosis.

As part of an effort to develop more specific biomarkers following local ablation of malignant tumors, we are currently exploring alternative methods to assess the success of ablation immediately after treatment. Such biomarkers may allow the identification of subsets of patients in which the therapy is only partially effective, and those patients would potentially benefit from additional local or systemic treatment. Furthermore, increasing the speed of such assessment may significantly improve the clinical outcomes in those patients treated by ablation.

In conclusion, the study demonstrated that YP1 is a very sensitive indicator of membrane permeability. Although this cannot be used as a specific surrogate indicator of cell death due to ablation, it may have a role in other oncologic applications that require membrane permeability for the delivery of cytotoxic therapies to target cancer cells. Further specific investigation should address whether YP1 may serve as an indicator of susceptible cells to such therapies.

Acknowledgments The current study was funded by NCI/R21 CA131763-01A1.

References

Abitabile P, Hartl U, Lange J, Maurer CA (2007) Radiofrequency ablation permits an effective treatment for colorectal liver metastasis. Eur J Surg Oncol 33:67–71. doi:10.1016/j.ejso.2006.10.040

Amersi FF, McElrath-Garza A, Ahmad A, Zogakis T, Allegra DP, Krasne R, Bilchik AJ (2006) Long-term survival after radiofrequency ablation of complex unresectable liver tumors. Arch Surg 141:581–587. doi:10.1001/archsurg.141.6.581

Boffa DJ, Waka J, Thomas D, Suh S, Curran K, Sharma VK, Besada M, Muthukumar T, Yang H, Suthanthiran M, Manova K (2005) Measurement of apoptosis of intact human islets by confocal optical sectioning and stereologic analysis of YO-PRO-1-stained islets. Transplantation 79:842–845. doi:10.1097/01.TP.0000155175.24802.73

Castañeda F, Kinne RKH (2000) Cytotoxicity of millimolar concentrations of ethanol on HepG2 human tumor cell line compared to normal rat hepatocytes in vitro. J Cancer Res Clin Oncol 126:503–510

Chagnon F, Fournier C, Charette PG, Moleski L, Payet MD, Dobbs LG, Lesur O (2010) In vivo intravital endoscopic confocal fluorescence microscopy of normal and acutely injured rat lungs. Lab Invest J Tech Methods Pathol 90:824–834. doi:10.1038/labinvest.2010.76

Chekeni FB, Elliott MR, Sandilos JK, Walk SF, Kinchen JM, Lazarowski ER, Armstrong AJ, Penuela S, Laird DW, Salvesen GS, Isakson BE, Bayliss DA, Ravichandran KS (2010) Pannexin 1 channels mediate 'find-me' signal release and membrane permeability during apoptosis. Nature 467:863–867. doi:10.1038/nature09413

Chiappa A, Makuuchi M, Lygidakis NJ, Zbar AP, Chong G, Bertani E, Sitzler PJ, Biffi R, Pace U, Bianchi PP, Contino G, Misitano P, Orsi F, Travaini L, Trifirò G, Zampino MG, Fazio N, Goldhirsch A, Andreoni B (2009) The management of colorectal liver metastases: expanding the role of hepatic resection in the age of multimodal therapy. Crit Rev Oncol Hematol 72:65–75. doi:10.1016/j.critrevonc.2008.11.003

Chow SC, Kass GEN, Orrenius S (1997) Purines and their roles in apoptosis. Neuropharmacology 36:1149–1156. doi:10.1016/S0028-3908(97)00123-8

Emmett DS, Feranchak A, Kilic G, Puljak L, Miller B, Dolovcak S, McWilliams R, Doctor RB, Fitz JG (2008) Characterization of ionotrophic purinergic receptors in hepatocytes. Hepatology 47:698–705. doi:10.1002/hep.22035

Gawlitta D, Oomens CW, Baaijens FP, Bouten CV (2004) Evaluation of a continuous quantification method of apoptosis and necrosis in tissue cultures. Cytotechnology 46:139–150. doi:10.1007/s10616-005-2551-7

Gillams AR (2005) The use of radiofrequency in cancer. Br J Cancer 92:1825–1829. doi:10.1038/sj.bjc.6602582

Gohla A, Eckert K, Maurer HR (1996) A rapid and sensitive fluorometric screening assay using YO-PRO-1 to quantify tumour cell invasion through Matrigel. Clin Exp Metastasis 14:451–458. doi:10.1007/BF00128961

Goldberg SN, Gazelle GS, Compton CC, Mueller PR, Tanabe KK (2000) Treatment of intrahepatic malignancy with radiofrequency ablation: radiologic-pathologic correlation. Cancer 88:2452–2463. doi:10.1002/1097-0142(20000601)88:11<2452:AID-CNCR5>3.0.CO;2-3

Gorodeski GI (2009) P2X7-mediated chemoprevention of epithelial cancers. Expert Opin Ther Targets 13:1313–1332. doi:10.1517/14728220903277249

Gwak JH, Oh BY, Lee RA, Chung SS, Kim KH (2011) Clinical applications of radio-frequency ablation in liver metastasis of colorectal cancer. J Korean Soc Coloproctol 27:202–210. doi:10.3393/jksc.2011.27.4.202

Hanley PJ, Kronlage M, Kirschning C, del Rey A, Di Virgilio F, Leipziger J, Chessell IP, Sargin S, Filippov MA, Lindemann O, Mohr S, Konigs V, Schillers H, Bahler M, Schwab A (2012) Transient P2X7 receptor activation triggers macrophage death independent of Toll-like receptors 2 and 4, caspase-1, and pannexin-1 proteins. J Biol Chem 287:10650–10663. doi:10.1074/jbc.M111.332676

Hanna NN (2004) Radiofrequency ablation of primary and metastatic hepatic malignancies. Clin Colorectal Cancer 4:92–100

Higashiyama S, Noda M, Kawase M, Yagi K (2003) Mixed-ligand modification of polyamidoamine dendrimers to develop an effective scaffold for maintenance of hepatocyte spheroids. J Biomed Mater Res Part A 64:475–482

Horbinski C, Mojesky C, Kyprianou N (2010) Live free or die: tales of homeless (cells) in cancer. Am J Pathol 177:1044–1052. doi:10.1111/j.1582-4934.2009.00832.x

Hur H, Ko YT, Min BS, Kim KS, Choi JS, Sohn SK, Cho CH, Ko HK, Lee JT, Kim NK (2009) Comparative study of resection and radiofrequency ablation in the treatment of solitary colorectal liver metastases. Am J Surg 197:728–736. doi:10.1016/j.amjsurg.2008.04.013

Idziorek T, Estaquier J, De Bels F, Ameisen JC (1995) YOPRO-1 permits cytofluorometric analysis of programmed cell death (apoptosis) without interfering with cell viability. J Immunol Methods 185:249–258. doi:10.1016/0022-1759(95)00172-7

Iglesias R, Locovei S, Roque A, Alberto AP, Dahl G, Spray DC, Scemes E (2008) P2X7 receptor-Pannexin1 complex: pharmacology and signaling. Am J Physiol Cell Physiol 295:C752–C760. doi:10.1152/ajpcell.00228.2008

Ito S, Itoga K, Yamato M, Akamatsu H, Okano T (2010) The co-application effects of fullerene and ascorbic acid on UV-B irradiated mouse skin. Toxicology 267:27–38. doi:10.1016/j.tox.2009.09.015

Jalilian I, Peranec M, Curtis BL, Seavers A, Spildrejorde M, Sluyter V, Sluyter R (2012) Activation of the damage-associated molecular pattern receptor P2X7 induces interleukin-1beta release from canine monocytes. Vet Immunol Immunopathol 149:86–91. doi:10.1016/j.vetimm.2012.05.004

Kim KH, Yoon YS, Yu CS, Kim TW, Kim HJ, Kim PN, Ha HK, Kim JC (2011) Comparative analysis of radiofrequency ablation and surgical resection for colorectal liver metastases. J Korean Surg Soc 81:25–34. doi:10.4174/jkss.2011.81.1.25

Kingham TP, Tanoue M, Eaton A, Rocha FG, Do R, Allen P, De Matteo RP, D'Angelica M, Fong Y, Jarnagin WR (2012) Patterns of recurrence after ablation of colorectal cancer liver metastases. Ann Surg Oncol 19:834–841. doi:10.1245/s10434-011-2048-x

Kohler JE, Dubach JM, Naik HB, Tai K, Blass AL, Soybel DI (2010) Monochloramine-induced toxicity and dysregulation of intracellular Zn 2+ in parietal cells of rabbit gastric glands. Am J Physiol Gastrointest Liver Physiol 299:G170–G178. doi:10.1152/ajpgi.00355.2009

Kuvshinoff BW, Ota DM (2002) Radiofrequency ablation of liver tumors: influence of technique and tumor size. Surgery 132:605–612. doi:10.1067/msy.2002.127545

Lee HY, Bardini M, Burnstock G (2000) P2X receptor immunoreactivity in the male genital organs of the rat. Cell Tissue Res 300:321–330

Liao SD, Puro DG (2006) NAD+-induced vasotoxicity in the pericyte-containing microvasculature of the rat retina: effect of diabetes. Invest Ophthalmol Vis Sci 47:5032–5038. doi:10.1167/iovs.06-0422

Liu SYW, Lee KF, Lai PBS (2009) Needle track seeding: a real hazard after percutaneous radiofrequency ablation for colorectal liver metastasis. World J Gastroenterol 15:1653–1655. doi:10.3748/wjg.15.1653

Livraghi T, Solbiati L, Meloni F, Ierace T, Goldberg SN, Gazelle GS (2003) Percutaneous radiofrequency ablation of liver metastases in potential candidates for resection: the "test-of-time" approach. Cancer 97:3027–3035. doi:10.1002/cncr.11426

Lupinacci R, Penna C, Nordlinger B (2007) Hepatectomy for resectable colorectal cancer metastases-indicators of prognosis, definition of resectability, techniques and outcomes. Surg Oncol Clin N Am 16:493–506. doi:10.1016/j.soc.2007.04.014

Manova K, Tomihara-Newberger C, Wang S, Godelman A, Kalantry S, Witty-Blease K, De Leon V, Chen WS, Lacy E, Bachvarova RF (1998) Apoptosis in mouse embryos: elevated levels in pregastrulae and in the distal anterior region of gastrulae of normal and mutant mice. Dev Dyn 213:293–308. doi:10.1002/(SICI)1097-0177(199811)213:3<293:AID-AJA6>3.0.CO;2-D

McArdle A, Maglara A, Appleton P, Watson AJ, Grierson I, Jackson MJ (1999) Apoptosis in multinucleated skeletal muscle myotubes. Lab Invest 79:1069–1076

Michel AD, Kaur R, Chessell IP, Humphrey PPA (2000) Antagonist effects on human P2X 7 receptor-mediated cellular accumulation of YO-PRO-1. Br J Pharmacol 130:513–520

Mishra A, Chintagari NR, Guo Y, Weng T, Su L, Liu L (2011) Purinergic P2X 7 receptor regulates lung surfactant secretion in a paracrine manner. J Cell Sci 124:657–668. doi:10.1242/jcs.066977

Misiakos EP, Karidis NP, Kouraklis G (2011) Current treatment for colorectal liver metastases. World J Gastroenterol 17:4067–4075. doi:10.3748/wjg.v17.i36.4067

Morimoto M, Sugimori K, Shirato K, Kokawa A, Tomita N, Saito T, Tanaka N, Nozawa A, Hara M, Sekihara H, Shimada H, Imada T, Tanaka K (2002) Treatment of hepatocellular carcinoma with radiofrequency ablation: radiologic-histologic correlation during follow-up periods. Hepatology 35:1467–1475. doi:10.1053/jhep.2002.33635

Mulier S, Ruers T, Jamart J, Michel L, Marchal G, Ni Y (2008) Radiofrequency ablation versus resection for resectable colorectal liver metastases: time for a randomized trial? An update. Dig Surg 25:445–460. doi:10.1159/000184736

Nishida K, Nakatani T, Ohishi A, Okuda H, Higashi Y, Matsuo T, Fujimoto S, Nagasawa K (2012) Mitochondrial dysfunction is involved in P2X7 receptor-mediated neuronal cell death. J Neurochem 122:1118–1128. doi:10.1111/j.1471-4159.2012.07868.x

Pulvirenti A, Garbagnati F, Regalia E, Coppa J, Marchiano A, Romito R, Schiavo M, Fabbri A, Burgoa L, Mazzaferro V (2001) Experience with radiofrequency ablation of small hepatocellular carcinomas before liver transplantation. Transplant Proc 33:1516–1517. doi:10.1016/S0041-1345(00)02577-X

Qu Y, Misaghi S, Newton K, Gilmour LL, Louie S, Cupp JE, Dubyak GR, Hackos D, Dixit VM (2011) Pannexin-1 is required for ATP release during apoptosis but not for inflammasome activation. J Immunol 186:6553–6561. doi:10.4049/jimmunol.1100478

Rai R, Richardson C, Flecknell P, Robertson H, Burt A, Manas DM (2005) Study of apoptosis and heat shock protein (HSP) expression in hepatocytes following radiofrequency ablation (RFA). J Surg Res 129:147–151. doi:10.1016/j.jss.2005.03.020

Santos F, MacDonald G, Rubel EW, Raible DW (2006) Lateral line hair cell maturation is a determinant of aminoglycoside susceptibility in zebrafish (Danio rerio). Hear Res 213:25–33. doi:10.1016/j.heares.2005.12.009

Siperstein AE, Berber E, Ballem N, Parikh RT (2007) Survival after radiofrequency ablation of colorectal liver metastases: 10-Year experience. Ann Surg 246:559–565. doi:10.1097/SLA.0b013e318155a7b6

Snoeren N, Jansen MC, Rijken AM, van Hillegersberg R, Slooter G, Klaase J, van den Tol PM, van der Linden E, Ten Kate FJW, van Gulik TM (2009) Assessment of viable tumour tissue attached to needle applicators after local ablation of liver tumours. Dig Surg 26:56–62. doi:10.1159/000194946

Snoeren N, Huiskens J, Rijken AM, Van Hillegersberg R, Van Erkel AR, Slooter GD, Klaase JM, Van Den Tol PM, Ten Kate FJW, Jansen MC, Van Gulik TM (2011) Viable tumor tissue adherent to needle applicators after local ablation: a risk factor for local tumor progression. Ann Surg Oncol 18:3702–3710. doi:10.1245/s10434-011-1762-8

Sofocleous CT, Klein KM, Hubbi B, Brown KT, Weiss SH, Kannarkat G, Hinrichs CR, Contractor D, Bahramipour P, Barone A, Baker SR (2004) Histopathologic evaluation of tissue extracted on the radiofrequency probe after ablation of liver tumors: preliminary findings. Am J Roentgenol 183:209–213

Sofocleous CT, Nascimento RG, Petrovic LM, Klimstra DS, Gonen M, Brown KT, Brody LA, Covey AM, Thornton RH, Fong Y, Solomon SB, Schwartz LH, Dematteo RP, Getrajdman GI (2008) Histopathologic and immunohistochemical features of tissue adherent to multitined electrodes after RF ablation of liver malignancies can help predict local tumor progression: initial results 1. Radiology 249:364–374. doi:10.1148/radiol.2491071752

Sofocleous CT, Petre EN, Gonen M, Brown KT, Solomon SB, Covey AM, Alago W, Brody LA, Thornton RH, D'Angelica M, Fong Y, Kemeny NE (2011) CT-guided radiofrequency ablation as a salvage treatment of colorectal cancer hepatic metastases developing after hepatectomy. J Vasc Interv Radiol 22:755–761. doi:10.1016/j.jvir.2011.01.451

Sofocleous CT, Garg S, Petrovic LM, Gonen M, Petre EN, Klimstra DS, Solomon SB, Brown KT, Brody LA, Covey AM, DeMatteo RP, Schwartz L, Kemeny NE (2012) Ki-67 is a prognostic biomarker of survival after radiofrequency ablation of liver malignancies. Ann Surg Oncol 19:4264–4269. doi:10.1245/s10434-012-2461-9

Solbiati L, Livraghi T, Goldberg SN, Ierace T, Meloni F, Dellanoce M, Cova L, Halpern EF, Gazelle GS (2001)

Percutaneous radio-frequency ablation of hepatic metastases from colorectal cancer: long-term results in 117 patients. Radiology 221:159–166

Sutherland LM, Williams JAR, Padbury RTA, Gotley DC, Stokes B, Maddern GJ (2006) Radiofrequency ablation of liver tumors: a systematic review. Arch Surg 141:181–190. doi:10.1001/archsurg.141.2.181

Taylor JM, Han Z (2010) Purinergic receptor functionality is necessary for infection of human hepatocytes by hepatitis delta virus and hepatitis b virus. PLoS One 5:e15784. doi:10.1371/journal.pone.0015784

Virginio C, Mackenzie A, North RA, Surprenant A (1999) Kinetics of cell lysis, dye uptake and permeability changes in cells expressing the rat P2X7 receptor. J Physiol 519:335–346. doi:10.1111/j.1469-7793.1999.0335m.x

Wang X, Sofocleous CT, Erinjeri JP, Petre EN, Gonen M, Do KG, Brown KT, Covey AM, Brody LA, Alago W, Thornton RH, Kemeny NE, Solomon SB (2013) Margin size is an independent predictor of local tumor progression after ablation of colon cancer liver metastases. Cardiovasc Intervent Radiol 36:166–175. doi:10.1007/s00270-012-0377-1

Xiao F, Waldrop SL, Khimji AK, Kilic G (2012) Pannexin1 contributes to pathophysiological ATP release in lipoapoptosis induced by saturated free fatty acids in liver cells. Am J Physiol Cell Physiol 303:C1034–C1044. doi:10.1152/ajpcell.00175.2012